Microfluidic Chips

DOI: 10.1002/ange.201404349

Integration of Platinum Nanoparticles with a Volumetric Bar-Chart Chip for Biomarker Assays**

*Yujun Song, Xuefeng Xia, Xifeng Wu, Ping Wang, and Lidong Qin**

Abstract: *Platinum nanoparticles (PtNPs) efficiently catalyze the transformation of H_2O_2 into oxygen gas. However, owing to the lack of an efficient approach or device that can measure the produced oxygen gas, the catalytic reaction has never been used for diagnostic applications. Microfluidics technology provides a platform that meets these requirements. The volumetric bar-chart chip (V-Chip) volumetrically measures the production of oxygen gas by PtNPs and can be integrated with ELISA technology to provide visible and quantitative readouts without expensive instrumentation or complicated data processing. Herein we show that PtNPs outperform catalase with respect to stability at high H_2O_2 concentrations or temperatures or in long-term reactions, and are resistant to most catalase inhibitors. We also show that the catalase-like activity of PtNPs can be used in combination with the V-Chip to sensitively and specifically detect cancer biomarkers both in serum and on the cell surface.*

Nanomaterials with applicable optical, electronic, magnetic, catalytic, and thermal properties play an important role in clinical diagnosis and medical management.[1] New emerging diagnostic technologies based on nanomaterials show great advantages over traditional methods, particularly in sensitivity, selectivity, and stability. These detection platforms rely on different types of colorimetric,[2] fluorescent,[3] electrochemical,[1b,c] Raman,[4] and magnetic[5] nanoparticles as transducers to convert molecular-recognition events into measurable outputs. Catalytic activity is another feature that has recently attracted great interest, as it can amplify a signal and increase detection specificity.[2b,6] Various nanoparticles have intrinsic catalytic activity and have been designed as catalytic labels for the sensitive and selective detection of proteins, nucleic acids, and other molecules.[6c] As highly efficient catalysts, platinum nanoparticles (PtNPs) have been used in medical applications, primarily diagnostics, for the detection of biomolecules by electrochemical or colorimetric methods.[7] However, for quantitative detection, expensive instruments are still required, which has limited their application. It has been shown that PtNPs are able to efficiently catalyze the reaction of H_2O_2 to generate oxygen gas.[7b] Owing to the lack of simple approaches or devices able to measure the end product (oxygen gas), the reaction has not been widely adopted for diagnostic applications.

Microfluidic chips allow portability, considerable throughput, and the capacity for integration with other diagnostic techniques for a complete, point-of-care device.[8] A volumetric bar-chart chip (V-Chip) has been developed with microfluidics technology to volumetrically measure the production of oxygen gas. This chip can be integrated with an ELISA reaction for quantitative detection of biomarkers, and the output consists of visible bar charts on the V-Chip, without any assistance from instruments, data processing, or graphic plotting.[9] In a previous iteration of this V-Chip, catalase was used as the ELISA probe to generate oxygen gas from hydrogen peroxide. However, several problems were encountered in this catalase-propelled microfluidic device. The drawbacks included the high cost of preparation and purification of catalase, its low operational stability owing to digestion and denaturation, and the dependence of catalytic activity on environmental conditions. The low catalytic stability leads to unsatisfactory sensitivity for V-Chip applications: Catalase is destroyed in the reaction with hydrogen peroxide,[10] and its activity is inhibited in the presence of high concentrations of H_2O_2.[9a]

Herein, we introduce PtNPs to the V-Chip platform (PtV-Chip) as a nanoparticle substitute for catalase (Figure 1). Our results indicate that PtNPs possess the requisite features, including excellent catalytic stability at high H_2O_2 concentrations and over long reaction periods, and the maintenance of activity over a broad temperature range and in the presence of catalase inhibitors. In this study, the PtV-Chip was used for quantitative and sensitive detection of the lung-cancer biomarker CYFRA 21-1 in a buffer and serum on the basis of standard sandwich ELISA. To demonstrate the breadth of potential applications, we performed on-chip cell culture and cell-based ELISA to detect human epidermal growth factor receptor 2 (HER2) and phosphorylated HER2 (pHER2) expression on the surface of breast-cancer cells.

PtNPs with an average diameter of 30 nm were prepared as previously described (see Figure S1 a,b in the Supporting

[*] Dr. Y. Song, Prof. X. Xia, Prof. P. Wang, Prof. L. Qin
Department of Nanomedicine,
Houston Methodist Research Institute
Department of Pathology and Genomic Medicine,
Houston Methodist Hospital
Department of Cell and Developmental Biology,
Weill Medical College of Cornell University
6670 Bertener Avenue, Houston, TX 77030 (USA)
E-mail: LQin@HoustonMethodist.org
Prof. X. Wu
Department of Epidemiology
The University of Texas M. D. Anderson Cancer Center
1155 Herman P. Pressler Boulevard, Houston, TX 77030 (USA)

[**] We are grateful for the support from NIH/NIDA 1R01DA035868-01, NIH/NCI 1R01CA180083-01, the Cancer Prevention and Research Institute of Texas (CPRIT-R1007), the Emily Herman Research Fund, and Golfers Against Cancer Foundation. We thank the HMRI scanning electron microscopy (SEM) core facility for instrumental assistance.

Supporting information for this article is available on the WWW under http://dx.doi.org/10.1002/anie.201404349.

 © 2014 Wiley-VCH Verlag GmbH & Co. KGaA, Weinheim

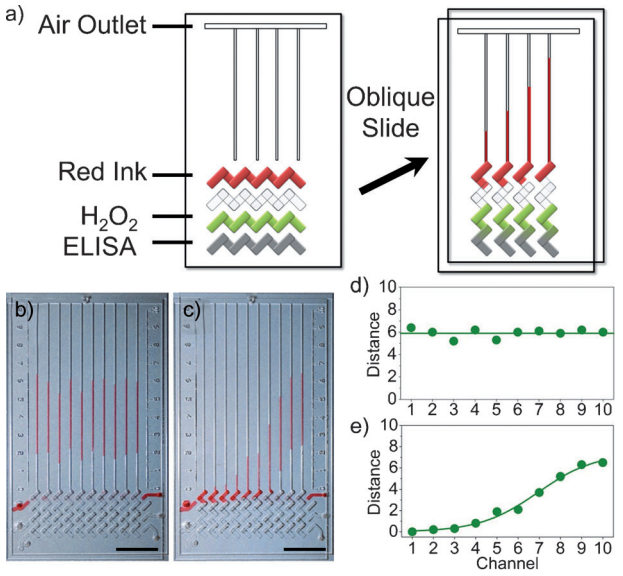

Figure 1. PtNPs have intrinsic catalase activity. a) Schematic view of a typical V-Chip for application in ELISA assays. Ink and H_2O_2 were preloaded, and the ELISA assay was performed in the designated lanes. An oblique slide breaks the flow path to form the structure on the right, thus causing PtNPs and H_2O_2 to react and push the ink up the channels. b,d) A uniform concentration of PtNPs (10 μg mL^{-1}) generates a uniform readout distance in the presence of 35% H_2O_2. c) Bar-chart image and e) corresponding graph showing the reaction of 35% H_2O_2 with PtNPs at different concentrations (diffusion gradient, 20 μg mL^{-1} in the initial solution). Scale bar for (b,c): 1 cm.

Information).[11] We first tested their catalase- and peroxidase-like activity by simply mixing PtNPs and H_2O_2. When PtNPs were added to H_2O_2, the characteristic "fizzing" was observed as a result of the production of oxygen gas (see Figure S1c). As well as catalase-like activity, PtNPs also possess intrinsic peroxidase-like activity (see Figure S2).[7b] In the presence of H_2O_2, PtNPs can catalyze the oxidation of peroxidase substrates to give a color reaction. The V-Chip provides a platform for quantitatively evaluating the production of oxygen gas. As shown in Figure 1b,c, when the PtNP solution was loaded in the V-Chip through the inlet holes, the ink-bar-chart movements correlated with the PtNP concentration. When a uniform PtNP concentration was used, the V-Chip showed uniform ink-bar-chart advancements (Figure 1b,d). When we created a diffusion gradient of PtNPs, the bar chart resembled a sigmoidal shape (Figure 1c,e). The progressive increments demonstrate the relationship between the height of the V-Chip bars and the PtNP concentration, thus indicating that the PtV-Chip can be used for quantitative biomarker detection.

To further examine the suitability of PtNPs as substitutes for catalase in the V-chip, we compared their performance in the 10-plex V-Chip. We used PtNPs or catalase diffusion in PBS buffer (phosphate-buffered saline) to study the kinetics of ink-bar-chart movements in each channel. The loading of 2 μL of PtNPs or protein into the preloaded PBS buffer in the bottom lane allowed the generation of a concentration gradient (see Figure S3). The movement of the ink bars was recorded with a camera (see the time-dependent distance of each channel at 10 min intervals in Figure S4). The images obtained clearly showed that the ink bar in the chip loaded with PtNPs moved much faster than that in the chip loaded with catalase at the same concentration. In 10 min, ten channels in the PtNP-loaded V-Chip formed clear ink bar charts, but only four channels formed ink bar charts in the catalase-loaded V-Chip. This result indicates that lower concentrations of PtNPs are required to produce readout from the V-Chip, and that the use of PtNPs improves the sensitivity of detection. Furthermore, the kinetics of ink-bar-chart movement clearly shows that PtNPs are catalytically stable over a longer reaction period. Figure 2a shows the time-dependent movement of the ink bar in the tenth channel: PtNPs exhibited a continuous increase in distance at 10 min, whereas catalase quickly reached a plateau in about 2 min, presumably as a result of degradation.[10]

An additional attractive feature of PtNPs is that they are catalytically stable over a broad H_2O_2-concentration range, which can be generated by allowing H_2O_2 to diffuse in preloaded water (Figure 2b). When 35% H_2O_2 (2 μL) was added to preloaded water to generate a concentration gradient, and the same concentration of PtNPs or catalase was then added, the ink-bar-chart patterns were different (see Figure S5). The pattern of the 10-plex V-Chip loaded with PtNPs had a sigmoidal shape, whereas the catalase-loaded chip resulted in a Gaussian shape, presumably owing to the inhibition of catalase activity at high concentrations of H_2O_2 (Figure 2c,d). It can be concluded that the optimal H_2O_2 concentration for the PtNP-mediated reaction is 35%, which provides more substrate for prolonged ink-bar-chart movement than catalase. Furthermore, PtNPs also show thermal stability at high temperature and resistance to most catalase inhibitors. As shown in Figure 2e, PtNPs retained 80% activity at 100 °C, whereas catalase completely lost its activity at 80 °C. We also studied the activity of PtNPs in the presence of six catalase inhibitors.[12] When a fivefold concentration of the inhibitor was used with PtNPs, only $NH_2OH{\cdot}HCl$ showed nearly complete inhibition of the activity of the PtNPs (Figure 2f). In contrast to catalase, PtNP activity only decreased slightly in the presence of NaN_3, which is a bacteriostatic agent widely used to preserve biological samples, such as commercialized antibodies.[13] Therefore, PtNP-conjugated antibodies do not need laborious or costly purification steps to remove NaN_3, which is another advantage over catalase.

Cytokeratin 19 fragments (CYFRA 21-1) are circulating tumor biomarkers with high specificity and sensitivity for non-small-cell lung cancer (NSCLC), particularly squamous cell carcinoma.[14] As an independent prognostic role, the serum level of CYFRA 21-1 can reflect the disease stage and treatment efficacy in NSCLC.[15] PtNPs were introduced in a single-channel V-Chip for the quantitative detection of human CYFRA 21-1. The fabrication and surface modification of the V-Chip were performed according to our previous method.[9] To detect CYFRA 21-1, we employed a typical three-component sandwich ELISA method (Figure 3), in which PtNPs were conjugated with the probe antibodies to react with the hydrogen peroxide and produce oxygen gas. We

© 2014 Wiley-VCH Verlag GmbH & Co. KGaA, Weinheim

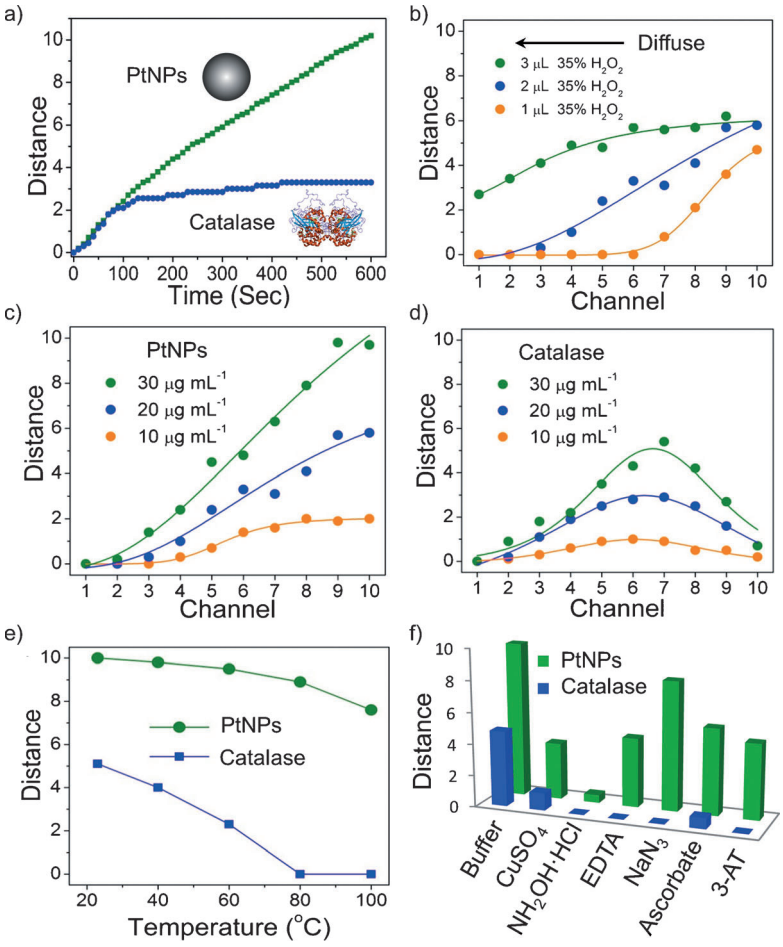

Figure 2. Comparison of PtNPs and catalase for the catalysis of oxygen-gas production in the 10-plex V-Chip. a) Time-dependent ink advancement with PtNPs and catalase at a concentration of 20 μg mL^{-1}. The H_2O_2 concentration was 35 and 4%, respectively. b) Bar-chart advancement after the diffusion of different volumes of 35% H_2O_2 in the presence of PtNPs (20 μg mL^{-1}). c,d) Bar-chart advancement upon the diffusion of 35% H_2O_2 (2 μL) in the presence of PtNPs (c) or catalase (d) at different concentrations. e) Catalytic activity of PtNPs and catalase after treatment at different temperatures for 30 min. f) Catalytic activity of PtNPs and catalase in the absence or presence of $CuSO_4$, $NH_2OH{\cdot}HCl$, ethylenediaminetetraacetic acid (EDTA), NaN_3, ascorbate, and 3-amino-1,2,4-triazole (3-AT). The concentration of the inhibitors was 25 mM and 5 mM for PtNPs and catalase, respectively.

tested a range of concentrations of CYFRA 21-1 (0.5–50 ng mL^{-1}) with the V-Chip (Figure 3c). Figure 3d shows the 10 min assay results from the test, in which the corresponding ink bar charts provide direct quantitative results of these concentrations. As the concentration of CYFRA 21-1 increased, the bar charts of the V-Chip exhibited a near-linear corresponding increase. In each case, the results obtained with solutions containing CYFRA 21-1 at a concentration of 0.5 ng mL^{-1} were greater by a factor of at least three standard deviations (SDs) than background signals, thus indicating that the limit of detection resides at or below this concentration. We also studied the ability of the PtV-Chip to detect CYFRA 21-1 under physiological conditions. When CYFRA 21-1 was spiked in serum at the same concentration, the bar-chart results exhibited a similar detection limit to that obtained with the buffer, thus indicating that serum matrices do not interfere significantly with PtV-Chip sensitivity (Figure 3e). The cutoff concentration of CYFRA 21-1 for the diagnosis of NSCLC in serum is 3.3 ng mL^{-1}.[14] Thus, the detection ability of the PtV-Chip is well within the range of clinical relevance for diagnosing NSCLC.

The rapid and sensitive detection of biomarker expression on cancer cells or tissues is particularly critical, as it not only can be used for the identification and classification of human tumors, but also provides approaches for selecting the most effective therapeutic targets to improve clinical outcomes. The traditional method for the detection of biomarker expression on cancer cells is based primarily on immunohistochemistry and fluorescence in situ hybridization.[16] Cell-based ELISA is an alternative rapid, convenient, and sensitive assay that is frequently used for measuring the relative amount of biomarkers and evaluating the effect of inhibitors, activators, or various treatments on cancer cells.[17] HER2 is a receptor tyrosine kinase that is detectable in a subset of breast or other adenocarcinomas and transitional cell carcinomas.[18] In the case of breast cancer, HER2 overexpression has been shown to be associated with poor prognosis, and is also a target for therapy.[18a]

To assess whether the PtV-Chip could be used for biomarker profiling, we cultured cells from three breast-cancer lines known to variably express HER2 (MDA-MB-231, MCF-7, and SKBR-3) in the assay wells of the bottom plate and assessed HER2 expression (Figure 4a). The rough surface of the assay wells modified with amino groups showed high adhesion with the cancer cells (see Figures S6–S8). After overnight incubation, cells were fixed and blocked with bovine serum albumin (BSA), and probe-antibody-conjugated PtNPs were loaded. Binding was assessed by the addition of H_2O_2. To demonstrate binding specificity, we used the peroxidase activity of PtNPs to catalyze the color reaction of 3,3′-diaminobenzidine (DAB) in the presence of H_2O_2, which would result in the staining of bound cells. MDA-MB-231 showed very little staining, MCF-7 was slightly stained, and SKBR3 showed strong staining (see Figure S9), which is consistent with previous reports.[9a] When approximately 1000 cells were seeded in each ELISA well, the quantitative results could be observed in the PtV-Chip results. If the distance values of HER2 on SKBR cells are considered to be 100% and it is assumed that the distance values are proportional to HER2 expression, MCF-7 cells expressed 13% HER2, whereas MDA-MB-231 showed almost no expression (Figure 4b,c). To calculate the sensitivity of V-Chip-based cell detection, different numbers of SKBR-3 cells were used. As the number of SKBR-3 cells increased, the V-Chip ink bar increased proportionally in size, thus suggesting an increased concentration of bound PtNPs. By using the

 © 2014 Wiley-VCH Verlag GmbH & Co. KGaA, Weinheim

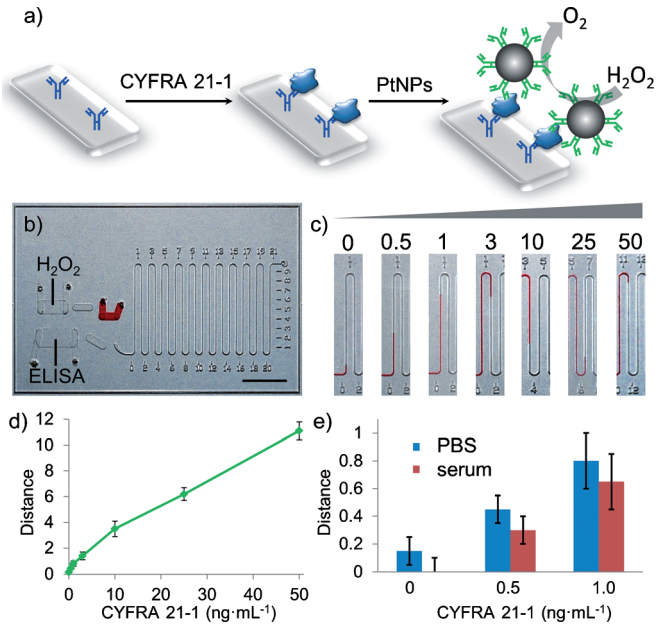

Figure 3. PtV-Chip for the detection of CYFRA 21-1. a) Standard sandwich ELISA was used in the PtV-Chip for biomarker detection. CYFRA 21-1 (blue) was added to the assay wells in the bottom plate and bound to the capture antibodies (blue). The PtNP–antibody complexes were loaded into the assay chamber to form sandwich structures. For detection of the target biomarkers, PtNPs were conjugated with the probe antibodies to react with the hydrogen peroxide and produce oxygen gas. b) Image of the PtV-Chip after the loading of reagents and samples. Scale bar: 1 cm. c) Images of singleplex V-Chip results in the absence or presence of CYFRA 21-1 at different concentrations (0.5, 1, 3, 10, 25, 50 ng mL^{-1}). d) CYFRA 21-1 calibration curve corresponding to ink advancement at 10 min, with CYFRA 21-1 concentrations of 0.5–50 ng mL^{-1}. e) Results for the detection of CYFRA 21-1 in PBS buffer and serum. The error bars in (d, e) represent the SD of three measurements.

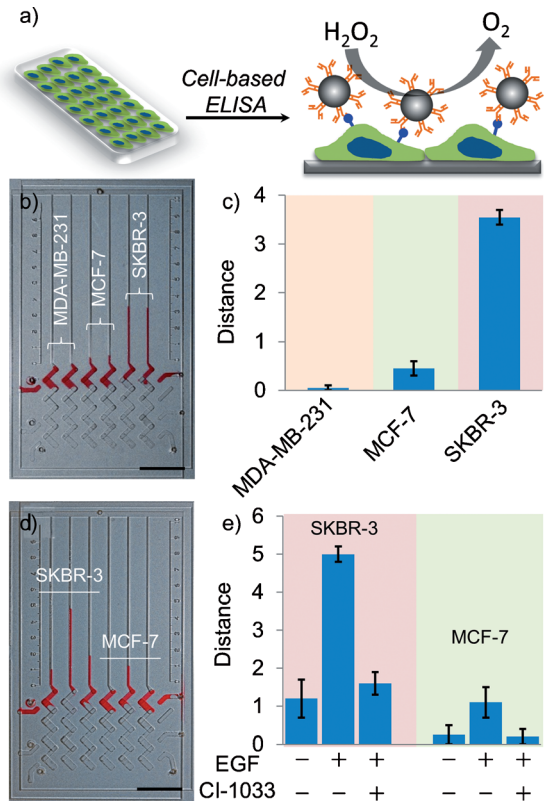

Figure 4. Cell-based ELISA for the detection of HER2 and pHER2 with the PtV-Chip. a) Schematic mechanism of cell-based ELISA for cell-surface biomarker detection with the PtV-Chip. Cells were seeded in the assay wells in the bottom plate. Antibody-conjugated PtNPs were used to target the cell-surface biomarkers and to react with the hydrogen peroxide to produce oxygen gas. b, c) PtV-Chip detection of HER2 expression on 1000 MDA-MB-231, MCF-7, and SKBR-3 cells. d, e) PtV-Chip detection of pHER2 expression on SKBR-3 and MCF-7 cells treated with or without EGF (100 ng mL^{-1}) and 5 mM CI-1033. Scale bar for (b, d): 1 cm. The error bars in (c, e) represent the SD of three measurements.

PtNP-incorporated V-Chip, we could detect as few as 400 SKBR-3 cells (see Figure S10).

Besides biomarker profiling, the PtV-Chip can also be used to detect protein phosphorylation. Protein phosphorylation plays important roles in the regulation of many cellular processes, including the cell cycle, growth, apoptosis, and signal-transduction pathways.[19] Because of its central importance to many biological processes, protein phosphorylation has been widely studied in attempts to understand its role in human disease.[20] Tyrosine phosphorylation on HER2 at position Y877 was investigated by using the cell-based ELISA method on the V-Chip. When SKBR-3 and MCF-7 cells were treated with epidermal growth factor (EGF; 100 ng mL^{-1}) for 1 h, HER2 phosphorylation was increased in both cell types (Figure 4 d,e).[21] To further investigate the phosphorylation state of HER2, we treated the cells with EGF and a small-molecule inhibitor, CI-1033. This molecule has been shown to irreversibly bind to the kinase domain of HER2.[21a] As shown in Figure 4 e, the tyrosine residue at position 877 was significantly dephosphorylated in the presence of 5 mM CI-1033.

In summary, the incorporation of PtNPs into the V-Chip enables the highly sensitive, quantitative, and instrument-free detection of protein biomarkers. As a V-Chip-based ELISA probe, PtNPs outperform catalase with respect to catalytic stability at high H_2O_2 concentrations over long reaction times, thermal stability at high temperatures, and resistance to most catalase inhibitors. Furthermore, PtNPs are a promising candidate as a catalase biomimetic and offer the advantages of ease of preparation and conjugation, low cost, and biostability. Owing to the high sensitivity of the PtNP-integrated V-Chip, disease-related biomarkers in serum or on the cell surface can be quantitatively and selectively detected.

Currently, diagnostic technologies are driven by the need to meet the requirements for point-of-care (POC) use in resource-limited settings.[22] Devices need to be sensitive, inexpensive, portable, and user-friendly to be adopted for wide-spread use. Although several microdevices with integrated microsensors for signal readout have been developed for biomarker quantitation through the miniaturization of conventional bulky instruments, most of these devices remain laboratory prototypes after a decade of development. Their commercial potential is limited because they are too costly,

© 2014 Wiley-VCH Verlag GmbH & Co. KGaA, Weinheim

too complicated to use, or not sensitive or specific enough to function in complex biospecimens (blood, serum).[22a,23] The study presented herein lays the foundation for PtNP-integrated V-Chips to be used in clinical diagnostics, drug screening, and environmental monitoring.

Received: April 15, 2014
Published online: July 17, 2014

Keywords: biomarker assays · catalytic activity · immunoassays · microfluidics · platinum nanoparticles

[1] a) N. L. Rosi, C. A. Mirkin, *Chem. Rev.* **2005**, *105*, 1547 – 1562; b) Y. Cui, Q. Wei, H. Park, C. M. Lieber, *Science* **2001**, *293*, 1289 – 1292; c) G. Zheng, F. Patolsky, Y. Cui, W. U. Wang, C. M. Lieber, *Nat. Biotechnol.* **2005**, *23*, 1294 – 1301; d) S. Laurent, D. Forge, M. Port, A. Roch, C. Robic, L. Vander Elst, R. N. Muller, *Chem. Rev.* **2008**, *108*, 2064 – 2110; e) X. Michalet, F. F. Pinaud, L. A. Bentolila, J. M. Tsay, S. Doose, J. J. Li, G. Sundaresan, A. M. Wu, S. S. Gambhir, S. Weiss, *Science* **2005**, *307*, 538 – 544; f) S. Lal, S. E. Clare, N. J. Halas, *Acc. Chem. Res.* **2008**, *41*, 1842 – 1851.

[2] a) R. Elghanian, J. J. Storhoff, R. C. Mucic, R. L. Letsinger, C. A. Mirkin, *Science* **1997**, *277*, 1078 – 1081; b) Y. Song, W. Wei, X. Qu, *Adv. Mater.* **2011**, *23*, 4215 – 4236.

[3] a) W. C. Chan, D. J. Maxwell, X. Gao, R. E. Bailey, M. Han, S. Nie, *Curr. Opin. Biotechnol.* **2002**, *13*, 40 – 46; b) S. Nie, Y. Xing, G. J. Kim, J. W. Simons, *Annu. Rev. Biomed. Eng.* **2007**, *9*, 257 – 288.

[4] a) Z. Chen, S. M. Tabakman, A. P. Goodwin, M. G. Kattah, D. Daranciang, X. Wang, G. Zhang, X. Li, Z. Liu, P. J. Utz, K. Jiang, S. Fan, H. Dai, *Nat. Biotechnol.* **2008**, *26*, 1285 – 1292; b) Y. C. Cao, R. Jin, C. A. Mirkin, *Science* **2002**, *297*, 1536 – 1540.

[5] R. S. Gaster, D. A. Hall, C. H. Nielsen, S. J. Osterfeld, H. Yu, K. E. Mach, R. J. Wilson, B. Murmann, J. C. Liao, S. S. Gambhir, S. X. Wang, *Nat. Med.* **2009**, *15*, 1327 – U1130.

[6] a) E. Katz, I. Willner, J. Wang, *Electroanalysis* **2004**, *16*, 19 – 44; b) L. Gao, J. Zhuang, L. Nie, J. Zhang, Y. Zhang, N. Gu, T. Wang, J. Feng, D. Yang, S. Perrett, X. Yan, *Nat. Nanotechnol.* **2007**, *2*, 577 – 583; c) I. Willner, B. Willner, *Nano Lett.* **2010**, *10*, 3805 – 3815; d) Y. Song, K. Qu, C. Zhao, J. Ren, X. Qu, *Adv. Mater.* **2010**, *22*, 2206 – 2210.

[7] a) R. Polsky, R. Gill, L. Kaganovsky, I. Willner, *Anal. Chem.* **2006**, *78*, 2268 – 2271; b) J. Fan, J. J. Yin, B. Ning, X. Wu, Y. Hu, M. Ferrari, G. J. Anderson, J. Wei, Y. Zhao, G. Nie, *Biomaterials* **2011**, *32*, 1611 – 1618.

[8] a) R. Fan, O. Vermesh, A. Srivastava, B. K. H. Yen, L. D. Qin, H. Ahmad, G. A. Kwong, C. C. Liu, J. Gould, L. Hood, J. R. Heath, *Nat. Biotechnol.* **2008**, *26*, 1373 – 1378; b) Y. Zhang, W. Zhang, L. Qin, *Angew. Chem.* **2014**, *126*, 2376 – 2380; *Angew. Chem. Int. Ed.* **2014**, *53*, 2344 – 2348.

[9] a) Y. Song, Y. Zhang, P. E. Bernard, J. M. Reuben, N. T. Ueno, R. B. Arlinghaus, Y. Zu, L. Qin, *Nat. Commun.* **2012**, *3*, 1283; b) Y. Song, Y. Wang, L. Qin, *J. Am. Chem. Soc.* **2013**, *135*, 16785 – 16788.

[10] P. George, *Nature* **1947**, *160*, 41 – 43.

[11] M. Huang, Y. Jin, H. Jiang, X. Sun, H. Chen, B. Liu, E. Wang, S. Dong, *J. Phys. Chem. B* **2005**, *109*, 15264 – 15271.

[12] a) D. Keilin, E. Hartree, *Nature* **1934**, *134*, 933; b) G. Arabaci, A. Usluoglu, *J. Chem.* **2013**, 6; c) A. J. Davison, A. J. Kettle, D. J. Fatur, *J. Biol. Chem.* **1986**, *261*, 1193 – 1200; d) G. Cohen, N. L. Somerson, *J. Bacteriol.* **1969**, *98*, 543 – 546.

[13] H. C. Lichstein, M. H. Soule, *J. Bacteriol.* **1944**, *47*, 221.

[14] B. Wieskopf, C. Demangeat, A. Purohit, R. Stenger, P. Gries, H. Kreisman, E. Quoix, *Chest* **1995**, *108*, 163 – 169.

[15] a) J. L. Pujol, O. Molinier, W. Ebert, J. P. Daures, F. Barlesi, G. Buccheri, M. Paesmans, E. Quoix, D. Moro-Sibilot, M. Szturmowicz, J. M. Brechot, T. Muley, J. Grenier, *Br. J. Cancer* **2004**, *90*, 2097 – 2105; b) R. T. Vollmer, R. Govindan, S. L. Graziano, G. Gamble, J. Garst, M. J. Kelley, R. H. Christenson, *Clin. Cancer Res.* **2003**, *9*, 1728 – 1733.

[16] I. T. Yeh, *Am. J. Clin. Pathol.* **2002**, *117*, 26 – 35.

[17] a) K. E. Foreman, A. A. Vaporciyan, B. K. Bonish, M. L. Jones, K. J. Johnson, M. M. Glovsky, S. M. Eddy, P. A. Ward, *J. Clin. Invest.* **1994**, *94*, 1147 – 1155; b) C. Y. Wu, J. T. Jan, S. H. Ma, C. J. Kuo, H. F. Juan, Y. S. Cheng, H. H. Hsu, H. C. Huang, D. Wu, A. Brik, F. S. Liang, R. S. Liu, J. M. Fang, S. T. Chen, P. H. Liang, C. H. Wong, *Proc. Natl. Acad. Sci. USA* **2004**, *101*, 10012 – 10017.

[18] a) Z. Mitri, T. Constantine, R. O'Regan, *Chemother. Res. Pract.* **2012**, 743193; b) Y. Ding, Z. Liu, S. Desai, Y. Zhao, H. Liu, L. K. Pannell, H. Yi, E. R. Wright, L. B. Owen, W. Dean-Colomb, O. Fodstad, J. Lu, S. P. LeDoux, G. L. Wilson, M. Tan, *Nat. Commun.* **2012**, *3*, 1271.

[19] P. Cohen, *Trends Biochem. Sci.* **2000**, *25*, 596 – 601.

[20] P. Cohen, *Eur. J. Biochem.* **2001**, *268*, 5001 – 5010.

[21] a) D. P. Hughes, D. G. Thomas, T. J. Giordano, K. T. McDonagh, L. H. Baker, *Pediatr. Blood Cancer* **2006**, *46*, 614 – 623; b) M. Gijsen, P. King, T. Perera, P. J. Parker, A. L. Harris, B. Larijani, A. Kong, *PLoS Biol.* **2010**, *8*, e1000563.

[22] a) Y. Song, Y.-Y. Huang, X. Liu, X. Zhang, M. Ferrari, L. Qin, *Trends Biotechnol.* **2014**, *32*, 132 – 139; b) P. Yager, G. J. Domingo, J. Gerdes, *Annu. Rev. Biomed. Eng.* **2008**, *10*, 107 – 144.

[23] V. Gubala, L. F. Harris, A. J. Ricco, M. X. Tan, D. E. Williams, *Anal. Chem.* **2012**, *84*, 487 – 515.

 © 2014 Wiley-VCH Verlag GmbH & Co. KGaA, Weinheim